ChemComm
Chemical Communications

Accepted Manuscript

This article can be cited before page numbers have been issued, to do this please use: J. I. Mendoza, F. C. Soncini and S. K. Checa, *Chem. Commun.*, 2020, DOI: 10.1039/D0CC01323D.

ROYAL SOCIETY OF CHEMISTRY

rsc.li/chemcomm

View Article Online
DOI: 10.1039/D0CC01323D

COMMUNICATION

Engineering of a Au-sensor to develop a Hg-specific, sensitive and robust whole-cell biosensor for on-site water monitoring

Julián I. Mendoza,[a] Fernando C. Soncini[ab] and Susana K. Checa[†ab]

Received 00th January 20xx,
Accepted 00th January 20xx

DOI: 10.1039/x0xx00000x

A highly sensitive and specific Hg-whole-cell biosensor was developed from a non-selective variant of the Au sensor GolS and its regulatory pathway. The performance of this analytical tool was validated under laboratory and field-like conditions. This biosensor can be easyly applied in cost-effective and portable semiquantitative devises to report Hg contamination in water.

Mercury (Hg) is listed among the top ten chemicals of major worldwide concern.[1, 2] Human activities such as mining, industrialization and improper deposition of electric and electronic waste, have increased the mobilization of this harmful and persistent element into the environment, especially in aquatic environments where it accumulates.[3-5] Prolonged exposure to Hg irreversibly damages the brain, kidney and other vital organs, and has teratogenic effects due to disturbance of fetal neurological development.[6] The most commonly used methods to quantify Hg (AAS, ICP) are highly sensitive but require expensive instrumentation, trained personnel and complex procedures.[3] This hinders routinely checking outside big cities, particularly in developing countries where controls on waste disposal are usually relaxed. Besides, these methodologies detect the total amount of Hg present in the samples without discriminating its bioavailability, the actual risk factor. Whole-cell biosensors (WCBs), genetically modified microorganisms coupling metal-sensor capacity to the production of a measurable output signal, provide information about bioavailability and emerge as a cost-effective, likely portable alternative to the current analytical methodologies.[7-10] In a typical biosensor platform, the main determinant of specificity and sensitivity is the sensor protein, whereas, the dynamic and operational ranges[‡] depend mainly on the proper design of the genetic circuit controlling reporter expression.[7, 8, 11] The central component of all reported Hg-WCBs is MerR, the cytoplasmic Hg^{2+} sensor/regulator protein that directs inorganic or organic mercury detoxification in bacteria.[12] Although MerR is remarkable sensitive to Hg^{2+} it lacks specificity because it can also respond to other harmful metal ions such as cadmium (Cd), gold (Au) or zinc (Zn).[13-15] Despite the application of synthetic biology tools to increase the sensitivity or the dynamic range of MerR-based WCBs [16-20], the specificity has not yet been improved, hindering their application to environmental sample analysis.

Previously, we built a broad-spectrum WCB capable of detecting water-soluble Hg with a sensitivity of 4.4 nM (eq to 0.9 ppb), as well as other toxic metals.[21] This analytical tool was based on GolS77, a non-specific variant of the MerR-like *Salmonella* GolS, and its highly efficient regulatory circuit, all assembled into a modular fluorescent biosensor platform. GolS77 carries a single S77C mutation. This adds a third ligand for metal coordination and allow this native Au^{+} sensor/regulator protein to respond also to Hg^{2+} and other divalent metals.[21, 22] The biosensor platform consists of: a) the sensor/transduction module, in this case, the chromosomally-encoded and self-regulated GolS77 regulator, and b) the reporter module, a plasmid carrying the *Aequorea victoria*'s green fluorescent protein coding gene, *gfp*, under the transcriptional control of the GolS-dependent *golB* promoter (see Fig. 1A). When Hg^{2+} (or other inducer ion) reaches the bacterial cytoplasm, it interacts with GolS77 triggering its activation, which in turn induces its own expression as well as the expression of the fluorescent reporter.[21] This positive regulatory loop improves the dynamic range of this biosensor platform by decreasing background fluorescence in the absence of the inducer metals, a common problem observed in other WCBs.[8, 19, 23]

To increase GolS77 specificity toward Hg, we replaced its metal-binding loop (MBL), the region directing metal specificity in GolS [21, 24], for the equivalent region of two non-specific Hg-sensors: the MerR proteins from either *Pseudomonas aeruginosa* Tn-501 transposon or *Bacillus megaterium* (see ESI for details). We specially chose these well-characterized MerR homologues because they differ in both primary sequences and structure, even at the MBL.[25, 26] Notice also that the MBL of both sensors are one residue longer than the GolS77 MBL (Fig. S1A, ESI). The designed sensors were named GolS77-LRT or GolS77-LRB as they have the MBL from either Tn-501 or *B. megaterium* MerR sensors, respectively. The genes coding for GolS77-LRT or GolS77-LRB were initially introduced into

[a] Instituto de Biología Molecular y Celular de Rosario (IBR), Universidad Nacional de Rosario (UNR)-Consejo Nacional de Investigaciones Científicas y Técnicas (CONICET), Rosario, Argentina.
[b] Departamento de Microbiología, Facultad de Ciencias Bioquímicas y Farmacéuticas, UNR, Rosario, Argentina.

† checa@ibr-conicet.gov.ar.

Electronic Supplementary Information (ESI) available: Detailed experimental procedures and additional figures and tables. See DOI: 10.1039/x0xx00000x

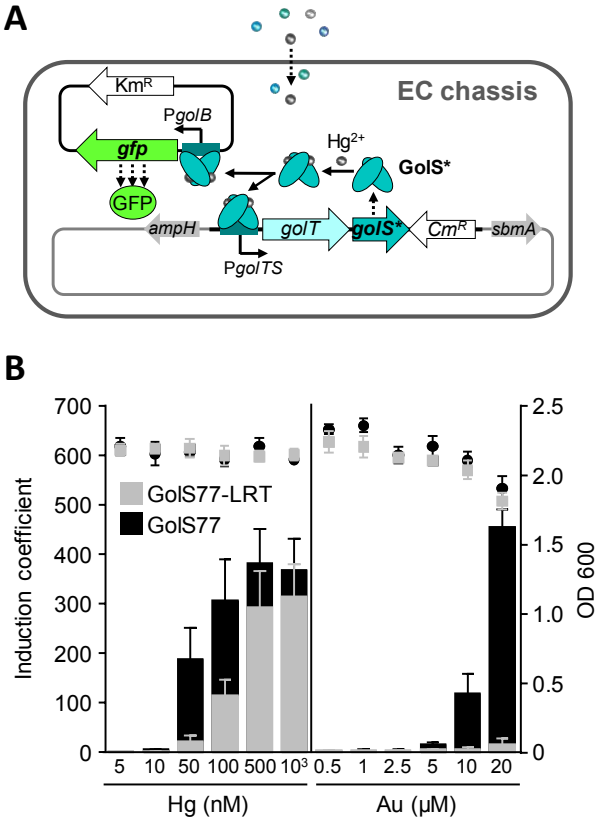

Fig. 1. The GolS77-LRT based WCB specifically detects Hg. (A) Schematic representation of the Hg-specific biosensor platform operating inside the EC chassis. The GolS77-LRT or the GolS77 coding gene, *golS**, and the GolT Au-transporter, *golT*, are co-transcribed from the GolS-dependent P*golTS* promoter. The plasmidic reporter construction P*golB-gfp* also depends on GolS (see details on Fig. S1 legend). The genes flanking the inserted *golT-golS**-Cm^R locus in the chromosome are indicated. The GolS77-LRT induction pathway is described in the text. (B) Response of the fluorescent GolS77-LRT and GolS77 based WCB after 4 h incubation in the presence of Hg or Au[§] ions. Details on the procedures are provided as ESI. Normalized fluorescence of the WCB in the absence of metal was calculated in 590 ± 68. This mean value was taken here as an induction coefficient (IC) of 1. Final optical density at 600 nm (OD 600) of each culture was included to evidence toxic effects. The data represent the mean ± SD of the IC or OD values obtained for four independent measurements done in triplicates.

the chromosome of a wild-type *S.* Typhimurium (STM) strain-the native GolS bacterial chassis[27]- carrying the GolS-dependent pPB-GFP reporter plasmid (Fig. S1B, ESI).

To test the ability of the synthetic GolS77-LRT or GolS77-LRB sensors to respond specifically to Hg, we measured the fluorescence emitted by the cells after 4 h incubation in the presence of increasing concentrations of Hg, Au, Pb, Cd or Co salts (see ESI for details). The strain expressing the GolS77 sensor was included as control.[§§] As shown in Fig. S2 (ESI), the output signal increased with $HgCl_2$ concentration in all cases, reaching similar levels at 1 μM $HgCl_2$. By contrast, only the GolS77-LRT reporter strain exhibited negligible activation by Au, at least at concentrations below 10 μM. Even at 20 μM $HAuCl_4$, a concentration that significantly affects bacterial growth, GolS77-LRT dependent induction reached only 20% of the values obtained in response to $HgCl_2$. As anticipated, Cd, Pb or Co ions did not significantly induce the reporter expression in any of the analysed strains (Fig S3, ESI). These data indicate that only coordination of Hg^{2+} at the GolS77-LRT metal binding site (Fig. S1A) drives productive conformational changes at the dimmer structure to activate transcription of the target promoters. The Hg-selectivity of the GolS77-LRT sensor can also be detected either in overnight cultures or in agar plates exposed to blue light, and correlates with the accumulation of the sensor protein in cell extracts (Fig. S4, ESI). These experiments also corroborate the proper functioning of the biosensor platform. To our knowledge, this is the first demonstration that the metal preference of a sensor protein can be tuned on-demand without significantly affecting its sensitivity, even for a metal ion that is not the native inducer of the system.

The excellent performance of GolS77-LRT to report Hg in the STM chassis prompted us to integrate this sensor/transduction module into the biosensor platform residing in a laboratory *Escherichia coli* (EC) strain[§§§] (Fig. 1A). As we previously reported [21, 23], optimal metal-detection using GolS-based EC biosensors requires self-regulation and the integration of the sensor coding gene into the bacterial chromosome, like in STM. Thus, we replaced in the chromosome of an engineered EC *golT-golS77* strain available in our laboratory, the *golS77* gene with the GolS77-LRT coding gene (see ESI for details). This strain also carries the pPB-GFP reporter plasmid (Fig. 1A). The response of the GolS77-LRT based WCB to $HgCl_2$ or $HAuCl_4$ was tested, using the parental GolS77-based biosensor as control (Fig. 1B). Final OD 600 was recorded in parallel to evidence toxic effects at high metal concentrations. As notice, maximal induction levels attained by both GolS77-LRT and GolS77-based EC biosensors were lower than in STM, the innate bacterial chassis (compared Fig. 1B and S2, ESI). This chassis-dependent effect has been previously noticed by us as well as by other authors [21, 23, 28-30], and could be attributed to differences in envelope permeability or intracellular metal handling. Surprisingly, in the EC chassis, the Hg-specificity of the GolS77-LRT sensor was significantly improved, as a consequence of a marked decrease in its response to Au compared with the GolS77-based WCB (Fig 1B). Furthermore, the calculated Hg/Au discrimination index for the GolS77-LRT sensor, that is the ratio between maximal induction attained with either metal, increased from 5 in STM, to 23 in the EC chassis.

Complete dose/response curves were done to better evaluated the response of the GolS77-LRT based WCB to $HgCl_2$ (Fig 2). The data was fitted to a three-parameter Hill equation to estimate the limit of Hg determination (LOD) as well as the dynamic and operational ranges of this analytical tool (see ESI for details). As shown in figure 2, the Hg-WCB tolerated up to 5 μM (~1000 μg L^{-1} or ppb) $HgCl_2$ without losing fluorescence or cell viability (Fig 2). Due to a very low leaky expression of the reporter construction (emitted fluorescence of ~200 RFU), a property of GolS-dependent platforms [21, 23], the designed WCB detects Hg with high sensitivity. The calculated LOD value was 20.4 nM Hg^{2+}, equivalent to 4.1 μg L^{-1} or ppb. This is higher than the estimated sensitivity of the non-specific GolS77-based or MerR-based biosensors [15, 20, 21, 31-35] but low enough to detect Hg contamination in water according to recommendations of the WHO[36] and other control agencies. The Hg-WCB exhibited also a remarkably wide dynamic range (k value in Fig. 2) with a ~300-fold increase at hight $HgCl_2$ concentrations and a linear response between 20 and 364 nM (eq. to 4-73 ppb) $HgCl_2$. Half maximal activation (K_M value in Fig. 2) was observed at 83 nM (16.7 ppb) $HgCl_2$. Comparing with other reported MerR-based biosensors [15, 20, 31-35], the GolS77-LRT based WCB does not require any sample

dilution or addition of external substrates, and has one of the widest operational and dynamic ranges.

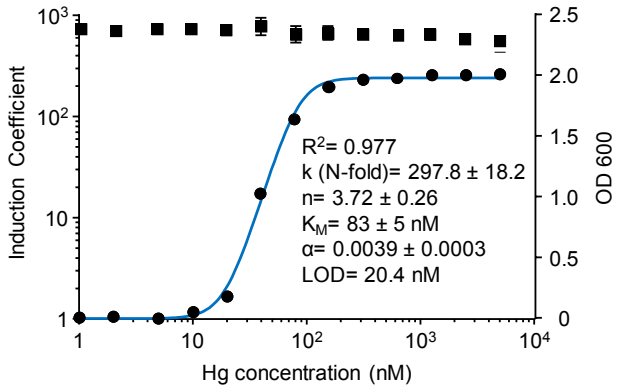

Fig. 2. The GolS77-LRT based WCB detects Hg in a wide range of concentrations. Emitted fluorescence and final OD 600 were measured in cells incubated during 4 hours with $HgCl_2$ (from 1 nM to 5 µM) and used to calculated the induction coefficient (IC) values. The mean of the IC values (circles) obtained at each concentration for five independent experiments done in triplicates was fitted to the Hill Function (solid blue line). The values of the relevant Hill function parameters (k, n, K_M and α), and the calculated R^2 and LOD values are also indicated. More details are provided in ESI. For OD 600 measurements (squares), the mean ± SD is indicated.

Based in these data and the lack of response to either Cd or Pb, other common water contaminants (Fig S5, ESI), we validate the use of the GolS77-LRT based WCB to specifically report and quantify bioavailable Hg in aqueous samples. First, we performed Hg determinations in water from different origins that were artificially contaminated with toxic metals (see ESI for details). We included in these assays: (i) ultrapure Milli-Q®, (ii) drinking water from the laboratory tap, or (iii) untreated high-salt, As-rich groundwater from a town nearby the highly populated and industrialized city of Rosario from the Argentine pampean plain. This region is known to be contaminated with arsenic and other trace metals/oids, but usually does not contain Hg.[37] Incubation of the Hg-WCB with water supplemented with $HgCl_2$ or different amounts of Cd, Pb or Au salts for 4 h provided similar values of fluorescence than those obtained when these metals were added directly to the bacterial cultures (compared Fig S6 (ESI) with Fig. 1B and S5). This served to validate the testing protocol. As expected from the Hg specificity of the designed WCB, no significant differences were observed in water samples supplemented only with Hg or with any of the Hg/Cd, Hg/Pb or Hg/Au mixtures (lower panel in Fig. S6, ESI).

Thinking in the future integration of this robust analytical tool into portable devices to perform on-site determinations, we tested the performance of the designed WCB to report Hg in water under field-like conditions, that is, at room temperature (25 ºC) and without shacking. In order to optimize the amount of biosensor bacteria needed to improve determinations under these conditions and perceive the output signal at short times, we dispensed different bacterial loads to Hg-contaminated groundwater. At different incubation times, the microplates were exposed to a blue-LED illumination in a dark room and photographed, but also introduced into a microplate reader to quantify the output signal and OD 600 (see ESI and Fig. S7 for details). Thus, we obtained both semiquantitative and quantitative information in parallel. As expected, fluorescence increased with time (Fig. 3). After 2 h of incubation, only the mixtures containing 1 x 10^8 CFU exhibited significant induction of the reporter (Fig. 3A). Nevertheless, the

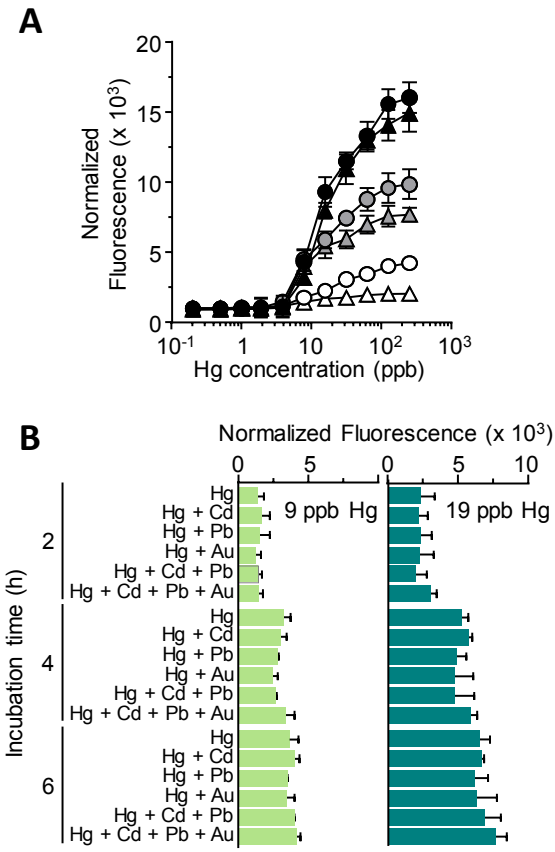

Fig. 3. Determination of bioavailable Hg in contaminated groundwater using the designed Hg-WCB under field-like conditions. (A) 5 x10^7 (triangles) or 1 x10^8 (circles) CFU of the Hg-WCB were mixed with groundwater supplemented with increasing amounts of $HgCl_2$ and incubated for 2 (white), 4 (grey) and 6 (black) hours at room temperature without shaking. These data also appear in Fig. S7B. (B) 1 x10^8 CFU of the Hg-WCB were mixed with groundwater supplemented with either 9 or 19 ppb Hg^{2+}(eq to 45 and 100 nM). When indicated, 5 µM of $CdCl_2$ (Cd), $Pb(NO_3)_2$ (Pb) and/or $AuHCl_4$ (Au) were also added. Emitted fluorescence and OD 600 were recorded at the indicated time to calculate the Normalized Fluorescence. The data represent the mean ± SD of four independent experiments done in triplicates.

fluorescence was still difficult to perceive with a naked eye (Fig. S8A, ESI). At 4 h, samples containing ≥7.8 ppb $HgCl_2$ and either 1 x 10^8 or 5 x 10^7 CFU showed an output signal that correlates well with the amount of metal added to the groundwater (Fig. 3A). From this data, LOD values of 4.7 and 5 ppb, respectively, were estimated. The increase in fluorescence of these samples can be easily perceived using a blue-LED transilluminator (Fig. S8, ESI). After 6 h of incubation, the output signal produced by samples containing either 1 x 10^8 or 5 x 10^7 CFU increased by a factor of at least two (Fig. 3A). At this time point, the increase in fluorescence was also similar in wells containing 2 x 10^7 CFU (Fig S8, ESI). In samples supplemented with lower amounts of the WCB, Hg-induced fluorescence was clearly perceived at longer incubation times (Fig. S7, ESI). However, irrespective of the bacterial load applied to the samples and the time required to achieve significant levels of the output signal, the sensitivity in Hg detection and the operational range of the WCB was preserved in all cases.

Further validation of the Hg-WCB performance was done on groundwater containing either 9 or 19 ppb $HgCl_2$ and supplemented in addition with $CdCl_2$, $PbNO_3$ and/or $HAuCl_4$ as indicated in Fig. 3B. These samples were inoculated either with 1 x 10^8 or 5 x 10^7 CFU and incubated at 2, 4 and 6 h, before fluorescence determination. As expected, bioavailable Hg was efficiently detected using the designed analytical tool, even in samples containing high amounts of other toxic metals (Fig. 3B).

The above results demonstrated the excellent performance of the GolS77-LRT-based WCB to report bioavailable Hg in water from 4 to >1000 ppb, even under conditions that a non-trained user could employed to perform on-site determinations or in a laboratory with minimal facilities. These properties also support the future integration of this robust analytical tool into portable devices for performing on-site Hg-screening in likely contaminated areas, contributing to increase the frequency of controls and prevent potential risks.

We thank Dr. Natalia Gottig for providing groundwater samples and helpful discuss of some of the results. J. M. is fellow of CONICET. S.K.C. and F.C.S. are career investigators of CONICET and Professors of the UNR. F.C.S. is also a career investigator of the Rosario National University Research Council (CIUNR). This work was supported by grants from Agencia Nacional de Promoción Científica y Tecnológica (PICT-2015-2339) to S.K.C.

Conflicts of interest

There are no conflicts of interest to declare.

Notes and references

‡ The dynamic range of the biosensor is the ratio between the highest and the lowest output signals measured. The operational range is the range of metal concentrations over which the biosensor exhibits a noticeable change in the output signal.[11]
§ Once inside the cytoplasm, Au^{3+} is rapidly reduced to Au^{+}.[38]
§§ In the wild-type STM strain, the GolS77 senses Hg^{2+} or Au^{+} but not to other divalent metals.[22]
§§§ This innocuous bacteria lacks the GolS regulatory circuit.[27]

1. WHO, Ten chemicals of major public health concern, https://www.who.int/ipcs/assessment/public_health/chemicals_phc/en/). (accessed February 2020)
2. ATSDR, 2017 Substance Priority List, https://www.atsdr.cdc.gov/SPL/#2017spl). (accessed February 2020)
3. D. O'Connor, D. Hou, Y. S. Ok, J. Mulder, L. Duan, Q. Wu, S. Wang, F. M. G. Tack and J. Rinklebe, *Environment International*, 2019, **126**, 747-761.
4. H. Hsu-Kim, K. H. Kucharzyk, T. Zhang and M. A. Deshusses, *Environmental Science & Technology*, 2013, **47**, 2441-2456.
5. S. A. Chiasson-Gould, J. M. Blais and A. J. Poulain, *Environmental Science & Technology*, 2014, **48**, 3153-3161.
6. G. Guzzi and C. A. M. La Porta, *Toxicology*, 2008, **244**, 1-12.
7. S. K. Checa, M. D. Zurbriggen and F. C. Soncini, *Current Opinion in Biotechnology*, 2012, **23**, 766-772.
8. H. J. Kim, H. Jeong and S. J. Lee, *Analytical and Bioanalytical Chemistry*, 2018, **410**, 1191-1203.
9. L. T. Bereza-Malcolm, G. Mann and A. E. Franks, *ACS Synthetic Biology*, 2015, **4**, 535-546.
10. B. Saltepe, E. Ş. Kehribar, S. S. Su Yirmibeşoğlu and U. Ö. Şafak Şeker, *ACS Sensors*, 2018, **3**, 13-26.
11. J. K. Rogers, N. D. Taylor and G. M. Church, *Current Opinion in Biotechnology*, 2016, **42**, 84-91.
12. T. Barkay, S. M. Miller and A. O. Summers, *FEMS Microbiology Reviews*, 2003, **27**, 355-384.
13. D. M. Ralston and T. V. O'Halloran, *Proceedings of the National Academy of Sciences*, 1990, **87**, 3846-3850.
14. K. M. Hakkila, P. A. Nikander, S. M. Junttila, U. J. Lamminmaki and M. P. Virta, *Appl Environ Microbiol*, 2011, **77**, 6215-6224.
15. A. Ivask, M. Virta and A. Kahru, *Soil Biology and Biochemistry*, 2002, **34**, 1439-1447.
16. M. Guo, R. Du, Z. Xie, X. He, K. Huang, Y. Luo and W. Xu, *Journal of Biological Engineering*, 2019, **13**, 70.
17. O. Wright, M. Delmans, G.-B. Stan and T. Ellis, *ACS Synthetic Biology*, 2015, **4**, 307-316.
18. B. Wang, M. Barahona and M. Buck, *Biosensors and Bioelectronics*, 2013, **40**, 368-376.
19. X. Wan, F. Volpetti, E. Petrova, C. French, S. J. Maerkl and B. Wang, *Nature Chemical Biology*, 2019, **15**, 540-548.
20. S. Cai, Y. Shen, Y. Zou, P. Sun, W. Wei, J. Zhao and C. Zhang, *Analyst*, 2018, **143**, 630-634.
21. S. Cerminati, F. C. Soncini and S. K. Checa, *Chem Commun (Camb)*, 2015, **51**, 5917-5920.
22. M. M. Ibáñez, S. K. Checa and F. C. Soncini, *J Bacteriol*, 2015, **197**, 1606-1613.
23. S. Cerminati, F. C. Soncini and S. K. Checa, *Biotechnol Bioeng*, 2011, **108**, 2553-2560.
24. M. M. Ibáñez, S. Cerminati, S. K. Checa and F. C. Soncini, *Journal of Bacteriology*, 2013, **195**, 3084-3092.
25. C.-C. Chang, L.-Y. Lin, X.-W. Zou, C.-C. Huang and N.-L. Chan, *Nucleic Acids Research*, 2015, **43**, 7612-7623.
26. D. Wang, S. Huang, P. Liu, X. Liu, Y. He, W. Chen, Q. Hu, T. Wei, J. Gan, J. Ma and H. Chen, *Scientific Reports*, 2016, **6**, 33391.
27. S. K. Checa and F. C. Soncini, *Biometals*, 2011, **24**, 419-427.
28. L. Bereza-Malcolm, S. Aracic and A. E. Franks, *Sensors (Basel)*, 2016, **16**, 2174.
29. T. Rijavec, J. Zrimec, F. Oven, M. K. Viršek, M. Somrak, Z. Podlesek, C. Gostinčar, A. Leedjärv, M. Virta, J. S. Tratnik, M. Horvat and A. Lapanje, *Geomicrobiology Journal*, 2017, **34**, 596-605.
30. L. Bereza-Malcolm, S. Aracic, R. Kannan, G. Mann and A. E. Franks, *Biosensors and Bioelectronics*, 2017, **94**, 380-387.
31. M. Virta, J. Lampinen and M. Karp, *Analytical Chemistry*, 1995, **67**, 667-669.
32. A. Ivask, K. Hakkila and M. Virta, *Analytical Chemistry*, 2001, **73**, 5168-5171.
33. T. Petänen, M. Virta, M. Karp and M. Romantschuk, *Microbial Ecology*, 2001, **41**, 360-368.
34. M. Pepi, D. Reniero, F. Baldi and P. Barbieri, *Water, Air, and Soil Pollution*, 2006, **173**, 163-175.
35. O. Selifonova, R. Burlage and T. Barkay, *Applied and Environmental Microbiology*, 1993, **59**, 3083-3090.
36. WHO, *Journal*, 2017.
37. S. S. Fańas, V. A. Casa, C. Vázquez, L. Ferpozzi, G. N. Pucci and I. M. Cohen, *Science of The Total Environment*, 2003, **309**, 187-199.
38. S. K. Checa, M. Espariz, M. E. Pérez Audero, P. E. Botta, S. V. Spinelli and F. C. Soncini, *Mol Microbiol*, 2007, **63**, 1307-1318.